Year 25, Issue 1 March, 1980

The SPEX Speaker

INDUSTRIES, INC. · 3880 PARK AVENUE · METUCHEN, N.J. 08840 · TEL (201) 549-7144

RAMAN SPECTROSCOPY AS AN INDUSTRIAL ANALYTICAL TECHNIQUE

C.A. Cody and R.K. Darlington
NL Industries, NL Chemicals
P.O. Box 700, Hightstown, N.J. 08520

Substantial literature has developed discussing the value of laser Raman spectroscopy for molecular structure determinations [1-3], classifying and characterizing polymers and deciphering polymer mechanics [4-6], tracking and elucidating solid state phase transitions [7-9], solving biological problems [10-12], etc. But there has been a disappointing lack of articles describing analytical applications of Raman spectroscopy to industrial problems. There is no valid reason for this absence of articles, as we will illustrate.

To support our contention, consider the fact that Raman spectroscopy offers the industrial community an analytical techniqne which is specific, accurate, rapid, requires little in the way of sample preparation and is, in many situations, highly sensitive. As an example of its specificity, the Raman spectrum of a typical organic compound will contain a large number of distinct spectral features. When excited, molecular groups, such as N-H, C-H, CH_2, CH_3, C = O, C-C, C-halogens, etc, produce spectral bands due to stretching, bending, twisting and torquing of these groups. Clearly, this wealth of spectral information may serve in a manner analogous and complimentary to infrared spectroscopy for specific and unique identification of organics. Furthermore, it is difficult to obtain infrared spectra in the $50cm^{-1}$ to $400cm^{-1}$ region, whereas this same region is easily recorded with modern laser-Raman instrumentation. This extended spectral region plus the band polarization information further strengthens the identification advantage of the Raman technique.

Inorganic functional groups also produce a number of unique Raman spectral features. The functional group frequencies vary for different phases of a single chemical compound, and vary from compound to compound as well. In solids the crystal-field effects slightly perturb these group frequencies, create or alter splittings, and change intensities so identification of Na_2SO_4 versus K_2SO_4 or $PbSO_4$, for example, is easily achieved. Since the Raman spectrum arises from the changing electronic polarizability during a molecular vibration [1], most Raman bands are spectrally narrow for ordered crystalline inorganic samples. This is an analytical advantage, compared to infrared analysis where strong dipolar couplings lead to extremely broad band widths for most inorganics. Another Raman advantage which helps to define the source of the spectral feature is the ease of obtaining Raman polarization data. Unfortunately, the application of Raman analysis to inorganics has been largely overlooked by the industrial community.

With the advent of modern photoelectric detectors, high resolution and high stray-light-rejection monochromators, and stable laser light sources, Raman spectroscopy has become an accurate and rapid quantitative analytical tool. Quantitative errors due to varying sample positions in the optical path of the instrument are minimized by internal standards. The ratio between the Raman signal of the sample and the signal of the internal standard is directly proportional to concentration, i.e. a linear curve is generated and requires no further corrections to serve as a calibration curve when it is obtained from prepared standards. An intense Raman spectrum can be recorded in 20-40 minutes and will cover the spectral range of $50cm^{-1}$ to $4000cm^{-1}$. Data in the $50cm^{-1}$ to $400cm^{-1}$ region can be especially valuable, particularly for inorganic and organometallic analyses.

Ease of sample preparation is another significant advantage of Raman spectroscopy as an analytical technique. Gaseous samples can be examined in optically transparent containers, and liquids or powders in small diameter glass capillary tubes. Large solid objects can be examined simply by placing a surface at the optical focus of the instrument.

As in most techniques, quantitative work requires internal standards; for gaseous samples either the strong N_2 symmetric stretch at $2238cm^{-1}$ or the O_2 symmetric stretch found at $1651cm^{-1}$ may be selected, though other diatomic or polyatomic gases may be preferable, depending upon the application. Suitable internal standards for liquid samples include liquids or solids which can be dissolved in the sample; the resulting solution is placed in capillary tubes or quartz ultraviolet/visible cells for spectral examination. Internal standards for solids could include $BaSO_4$, $CaCO_3$ or solid organics. These are powdered with the sample, and the entire mixture examined as pressed pellets or as loosely packed powders in capillary tubes. Sampling accuracy can be improved by defocusing the laser beam and/or rapidly rotating the pellet.

The intrinsic Raman intensities of molecular vibrations vary greatly as different chemical groups or molecules are encountered [13]. This variance in intensity can identify specific chemical groups in the presence of others or serve to extend the quantitative analytical detection of one species in another. For instance, covalent bonds such as S-S, S-H, N-H, C = C and C ≡ C tend to produce proportionally stronger signals than C-C, C-H or ionic bonds such as O-H; these same covalent bonds are weak or non-existent absorbers in the infrared spectrum. Raman detection of N-H in the

presence of O-H is easily accomplished, but is difficult with infrared spectroscopy. The analogous situation is true for inorganics, for example: the symmetric stretch of NO_3 is usually not seen in the infrared but is a strong Raman spectral feature. It becomes almost mandatory, then, that both infrared and Raman examinations are carried out for a complete sample characterization.

Organics and inorganics dissolved in water provide the best illustration of the variance in Raman intensity with chemical functionality. The large degree of ionic bonding in water produces a very weak Raman spectrum so that additives or impurities can be seen at parts per million concentrations in aqueous media. Thomas [14] has reported, for instance, detection of dimethylnitrosamine in water at concentrations as low as 10 mg per liter (10 ppm). As another example, the metal-carbon-sulfur or -nitrogen bonds in organometallic compounds produce strong Raman signals. The intensity of organometallic bands can be several to many times the intensity of bands due to C-C or C-H skeletal motions.

Mention must be made of the major disadvantage of Raman analysis; that is, the possible presence of a strong fluorescent background. This fluorescence is thought to arise from minor impurities which absorb the exciting radiation then emit photons at lower energies. Although in extreme instances the fluorescence can totally obscure the superimposed Raman signal, this has rarely been encounterd in our laboratory where the more prevalent situation is a fluorescent background of approximately the same strength as the Raman signal. There are methods to deal with this interference which include recrystallization of solids, filtering liquids through activated charcoal, changing to lower energy laser excitation frequencies, laser quenching, additive quenching or Raman gain experiments such as those described by Nestor [15]. The point to note is that the occasional presence of fluorescent backgrounds can usually be dealt with and will rarely eliminate Raman analysis.

In this article we discuss some typical industrial analytical problems and their solutions based upon Raman spectroscopy. Examples were selected to illustrate each of the above-stated advantages. Emphasis is placed on fast and accurate analysis for solving industrial analytical problems. We stress the fact that only ordinary Raman techniques were applied. All of the results were obtained with a SPEX 1401 monochromator, Coherent Radiation model 52A Argon ion laser (5145A, 2 watts maximum power), a Keithly Instruments 414S picoammeter with dc detection, a FW-130 photomultiplier tube and a Hewlett-Packard 7101B strip chart recorder. A SPEX SCAMP data system was incorporated for band integration or background subtraction to improve accuracy.

Thermal chemistry of antimony oxides and lead carbonate

Antimony oxides exist in several different compositions and also display polymorphism. The two common forms of Sb_2O_3 are the cubic phase (senarmontite) and the orthorhombic phase (valentinite). [16-18]. The polymorphic forms of Sb_2O_4 are the orthorhombic α phase (cervantite) and a high-temperature monoclinic

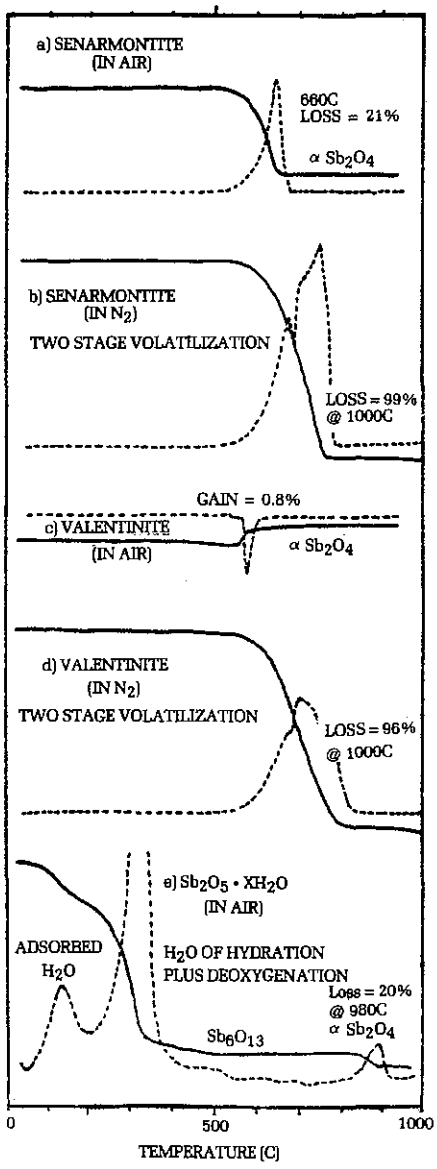

Figure 1 Thermolysis curves for various antimony oxides [21] demonstrate the changing weight of samples as a function of temperature during outgasing (solid curves) but do not characterize the components. However, recording the Raman spectra for residues along each thermal curve yields unambiguous identification (Figure 2). Traces a through d were heated at 20C/min, trace e at 50C/min. Dotted lines are the first derivatives of weight changes. (Reprinted by permission of the American Chemical Society.)

β phase [22]. Antimonic acid can be best described as $Sb_2O_5 \cdot XH_2O$; its dehydration and thermal decomposition product being Sb_6O_{13}, i.e., $Sb_2O_{4.35}$. Further heating of Sb_6O_{13} yields Sb_2O_4 as the final composition [20].

Several of the antimony oxides find application as commercial flame-retardant additives in chlorine-containing plastics. Properties of importance when incorporated into a plastic include oxygen index (oxygen composition at which burning is self-sustaining), high or low tint strength (optical hiding power), hardness (abrasiveness to plastics) and heat stability (stability during processing). To optimize these properties, the most important variables to control during manufacture of antimony oxide are the chemical and crystal-structure purity. This is essential because some of the oxide compositions and/or polymorphs do not function as flame retardants and, even more significantly, their presence, even at low concentrations, can be extremely detrimental to the additive's performance.

The exact mode of formation and thermal interconversion of crystal structures or oxidation states were not well understood before we began our study. Nor were there analytical techniques described in the literature for detecting one composition or polymorph in another below ~5 weight %. By combining Raman spectroscopic examination with thermal analysis, we were able to solve both problems simultaneously [21, 23].

Typical thermogravimetric analysis curves obtained when antimony oxides were heated in air or nitrogen are displayed in Figure 1. Raman spectra were recorded of milligram-size residues from each stable plateau region of the thermal curve. Because each polymorph of a particular oxidation state gives rise to a unique Raman spectrum, a rapid and complete qualitative characterization of the thermal chemistry of antimony oxides was achieved. Raman spectra of the various oxides are presented in Figures 2 and 3.

Raman spectra of Sb_2O_3 above its melting point were obtained by placing Sb_2O_3 powder in a 2mm fused-silica capillary tube wrapped with fine Nichrome wire. The wire was connected to a Variac to control the temperature and a chromel-alumel thermocouple placed in contact with the powder or melt to record the temperature. The spectrum of Sb_2O_3 liquid obtained in this manner (Figure 3) revealed that the extensive Sb-O chain structure found in valentinite (Sb_2O_3) was also present in the liquid. Quenching of the melt always led to valentinite, leading us to conclude that it is not com-

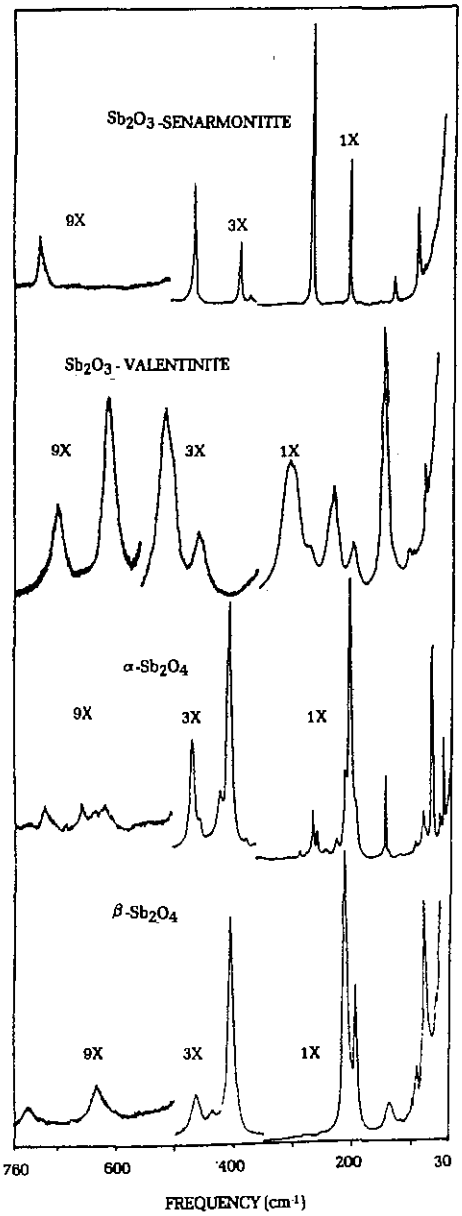

Figure 2 Raman spectra of polycrystalline senarmontite, valentinite, α-Sb_2O_4, and β-Sb_2O_4 [21] which corresponds to the residues of samples shown in the TGA curve of Figure 1. Resolution is $1cm^{-1}$. (Reprinted by permission of ACS.)

mercially feasible to produce forms other than valentinite via a Sb_2O_3 melt process.

A thin-walled fused-silica capillary tube as a sample holder for obtaining high temperature Raman spectra has several advantages and serves to illustrate the simplicity of sample handling in Raman spectroscopy. First, only a few milligrams of sample are needed to produce a high signal-to-noise spectrum; this is important for samples which are volatile, corrosive, poisonous or explosive. Second, melts can be viewed by passing the laser beam through the tube and melt, with only a small amount of absorption occurring due to the short traverse path of the beam. Third, any sample holder at temperatures above ~800C becomes a strong black-body radiator in the visible region, leading to high spectral background levels. The small surface area of the capillary tube furnace helps to minimize the intensity of the black-body background. Fourth, each tube is inexpensive and easily prepared. Fifth, a tube can be readily heat sealed for permanent sample storage. Sixth, the silica spectral bands are weak and will not generally interfere with the recording of spectra. Finally, the assembly is stable to ~ ± 10C in a draft-free sample compartment.

Antimony oxide literature was inconclusive as to whether α- or β-Sb_2O_4 was produced from the thermal decomposition of $Sb_2O_5 \cdot XH_2O$ [20, 22]. To resolve this question, residues from thermogravimetric analysis at atmospheric pressure were examined along with residues produced by heating $Sb_2O_5 \cdot XH_2O$ in sealed capillaries at elevated pressures. These experiments led to the conclusion that α-Sb_2O_4 was the stable low pressure decomposition product and β-Sb_2O_4 was the stable decomposition product at elevated pressures. Thus, to produce the β phase commercially, a thermal reactor would have to operate at elevated pressures.

Raman spectroscopy was also chosen to monitor common impurities and phases causing detrimental additive performance in commercial products. The spectroscopic procedure for quantitation of impurities in senarmontite involves obtaining the ratio of an impurity peak to a senarmontite peak. Plots of various impurity or phase peak heights at known concentrations then become calibration curves.

Standards must be homogeneous because the laser beam stimulating the Raman spectra is focused to a very small area. Non-homogeneous samples cause differing band heights as one moves to different regions of the same sample. To assure homogeneity, each standard was mixed with fine granular KBr (at ~1:1 weight ratio), enclosed in a stainless-steel capsule and agitated at high speed for one minute. The mixture was then ground, in the same capsule, at high speed with a carbide ball for one minute, before being pressed into a 13mm disc at 12 tons/sq. in. Homogeneity was checked by recording Raman spectra on several sections of each standard until mixing and grinding resulted in a constant band height. This method also helps to eliminate particle-orientation effects. Rotation of the KBr pellet (700-1000 rpm) would help to further average out simple variations and preferred orientation. Specific detection limits were below 0.5 weight % for

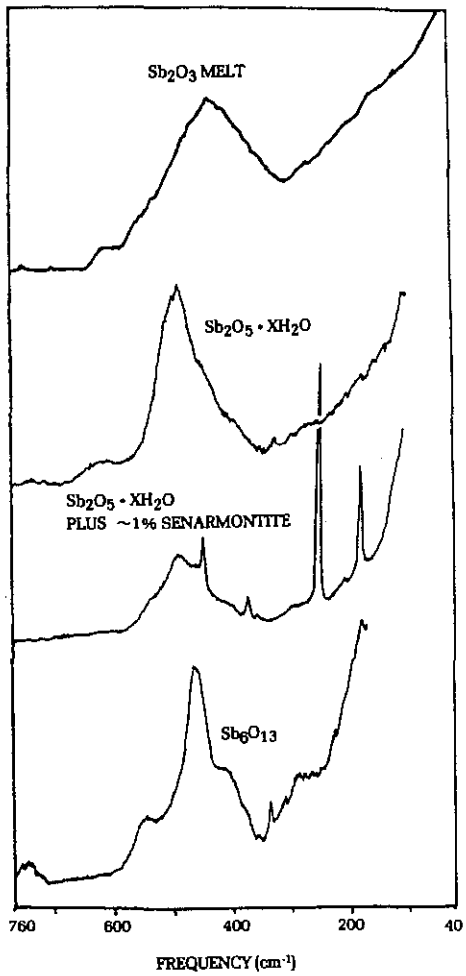

Figure 3 Raman spectra of Sb_2O_3 melt, polycrystalline $Sb_2O_5 \cdot XH_2O$, $Sb_2O_5 \cdot XH_2O$ with ~1% senarmontite, and Sb_6O_{13} [21], recorded with $4cm^{-1}$ resolution. Figures 1-3 demonstrate the power of combining TGA and Raman spectroscopy into a qualitative and quantitative technique. (Reprinted by permission of ACS.)

As_2O_3, PbO, valentinite, and 1.0 weight % for α-Sb_2O_4 in senarmontite [23].

The extreme variance in Raman intensity with compound type or chemical functionality is often advantageous for quantifying impurities. This holds true when weak spectral bands from the bulk sample can be measured as internal standard bands, i.e. are weakly scattering, and the impurity of interest is a strong Raman scatter. The weak spectrum of the principal component minimizes errors by allowing ratioing bands of similar intensities. One such example is the weak Raman spectrum from $Sb_2O_5 \cdot XH_2O$ which extends the quantitation limits of the strong Raman scattering senarmontite (Sb_2O_3) impurity. To illustrate this, the spectra of 1.0 weight % senarmontite in $Sb_2O_5 \cdot XH_2O$ is given in Figure 4. Quantitative measurement of as little as 0.01 weight percent senarmontite in $Sb_2O_5 \cdot XH_2O$ was successful. A similar procedure enabled Capwell et al [24] to report detection of as little as 0.03% anatase (TiO_2) in rutile (TiO_2).

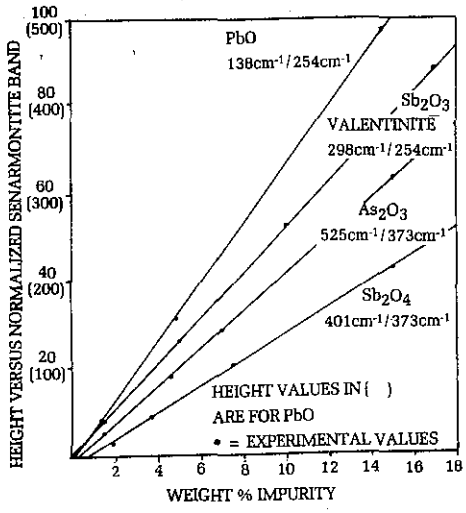

Figure 4 Calibration curves for weight % impurity versus senarmontite (Sb_2O_3) band height adjusted to 100 units. The first frequenty listed is for the impurity, the second for senarmontite. In contrast to techniques such as X-ray diffraction or infrared spectroscopy, Raman spectroscopy provides a method of fast, precise quantitation, linear over several decades of concentration and sensitive to fractions of a percent for individual phases of inorganic compounds.

degraded. The thermal decomposition of $PbCO_3$ in air begins at 225C and is complete by 430C [23]. The final product is PbO. The derivative of weight loss versus temperature indicates three CO_2 volatilization rates. The major rate changes occur at 350C and 390C, suggesting changes in crystal structure at these temperatures. Raman spectroscopy confirms the thermal results and so provides an explanation for CO_2 volatilization rates. When combined, the thermal and Raman analyses also explain why $XPbO \cdot YPbCO_3$ performance varies with stoichiometry.

Gas analysis

Raman spectroscopy is especially effective for analyzing gases evolved during chemical reactions and thermal decompositions, for monitoring plant effluents, or for probing the atmostphere above air-sensitive samples. To illustrate one interesting combination with thermal analysis, we followed the loss of SO_2 during thermal decomposition of $NaHSO_3$. A DuPont 990 Thermal Analyzer (TGA) monitored the thermal decomposition; nitrogen gas at a flow rate of 50 ml/minute purged the unit. The N_2 gas, along with SO_2 from the decomposition of $NaHSO_3$, was swept via a 3' x 1/2" Tygon tube toward the optical focus of the Raman instrument. The exit end of the Tygon tubing was ~1/16" from the focal point. By setting the monochromator on the SO_2 symmetric stretch band at 1151cm^{-1}, a curve of SO_2 intensity versus temperature was obtained (Figure 6A). This curve represents the instantaneous SO_2 concentration versus temperature of $NaHSO_3$. A SPEX SCAMP data system calculated the indefinite integral of this curve (Figure 6B), which represents the accumulated SO_2 concentration. At this point standard N_2/SO_2 mixtures could be examined to determine the total SO_2 weight lost. We did not carry out this aspect of the experiment. However, to illustrate its effect, the SCAMP was instructed to subtract a 25.6% weight of SO_2 from a 100% line representing the starting weight of $NaHSO_3$. This generates a pseudo weight loss versus temperature curve (Figure 6C). For comparison, the actual weight loss curve obtained from the DuPont 990 during the TGA run is presented in Figure 6D.

Comparison of curves C&D in Figure 6 reveals a slight temperature displacement of curve C toward higher temperature due to the finite flow time of N_2 and SO_2 through the apparatus, (if needed,

Figure 6 SO_2 evolution measured by Raman spectroscopy during thermal decomposition of $NaHSO_3$. Curve A. real-time SO_2 intensity; B. cumulative SO_2 intensity; C. weight loss curve for sample after subtracting SO_2 loss; D. TGA curve. Although only one effluent is illustrated, Raman spectroscopy can continuously measure many effluents, including N_2, O_2 and Cl_2.

Raman spectroscopy is also useful for examining finished products containing antimony oxides or other inorganic or organic additives. Figure 5 presents a portion of the Raman spectrum of semi-rigid polyvinyl chloride (PVC) and PVC containing ~1.0 weight % antimony oxide. Even at this additive level impurities in the Sb_2O_3 can be determined as well as the percent Sb_2O_3. Again, this type of finished product analysis is enhanced when strongly scattering additives or impurities are contained within a weakly Raman-scattering sample.

Lead carbonate, $PbCO_3$, and some of its thermal decomposition products ($XPbO \cdot YPbCO_3$) have numerous commercial applications, including additives for paints and ceramics, and stabilizers for plastics. Decomposition products of lead carbonate are thought to be well defined only at certain stoichiometric compositions, such as $PbO \cdot PbCO_3$ (white lead) or $2PbO \cdot PbCO_3$ (dibasic lead carbonate), although performance can actually be maximized at other compositions. One analytical task in commercial manufacturing is monitoring the exact $PbO/PbCO_3$ ratio during production. Raman spectroscopy offers an ideal solution to this problem: by taking the ratio of the height of the PbO band against that from $CO_3^{=}$, the composition can be determined for most products of interest.

Raman examination also provides an explanation for the mechanism of CO_2 volatilization when $PbCO_3$ is thermally

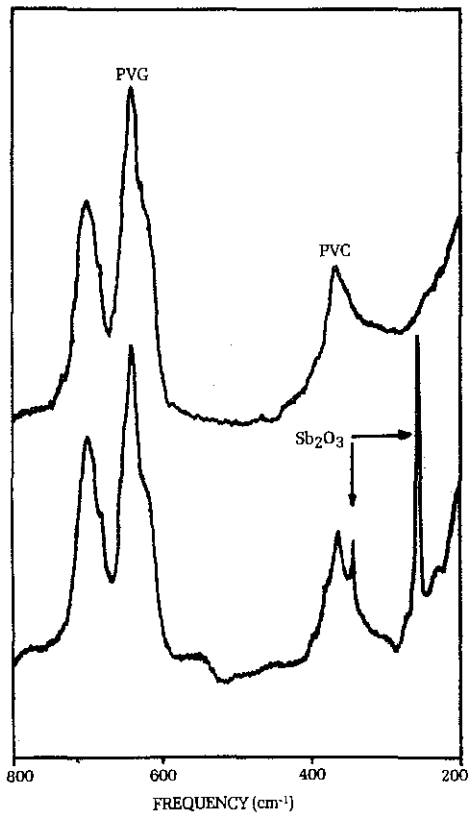

Figure 5 Raman spectra of polyvinyl chloride (PVC) and PVC containing ~1 weight % senarmontite (Sb_2O_3), a common fire retardant additive. Raman spectroscopy has proved to be an excellent technique for determining other inorganic additives in plastics, such as stebilizers, anti-oxidants, pigments, extenders, strengtheners, etc.

a correction term can be applied) and a slight rounding of curve C caused by the back mixing of SO_2 with N_2 in the thermal instrument. The sensitivity of SO_2 detection is very high; with 82 mg of $NaHSO_3$ a total of 21 mg of SO_2 (25.6%) is evolved and subsequently detected over a span of 100C. Should even better sensitivity be desired, a gain could be realized by multi-passing the laser beam through the gas.

The combination of Raman and thermal analysis for gaseous species is noteworthy for a number of reasons. First, the ability to determine off-gases quantitatively during thermal analysis is important because it allows one to decipher a thermal-loss curve that is due to the simultaneous loss of several gaseous species. Second, Raman spectroscopy can detect and determine quantitatively homonuclear diatomics such as N_2, O_2, H_2, etc which infrared spectroscopy cannot. (In thermal analysis, species like N_2 or O_2 are encountered quite often.) Third, although gas chromatography will also rapidly analyze and quantitatively measure gases, Raman does so continuously as a function of temperature. Fourth, Raman spectroscopy can examine milligram-size residues from the TGA experiment.

The value of this last point can be seen by noting that the Raman spectrum of the residue produced by heating $NaHSO_3$ in N_2 to 1000C is that of Na_2SO_4. The spectrum is of a metastable phase, however, and not that of the "normal" phase found for anhydrous Na_2SO_4. The detection of this metatable crystal phase suggested a short study of phase transitions in Na_2SO_4 and $Na_2SO_4 \cdot 10H_2O$.

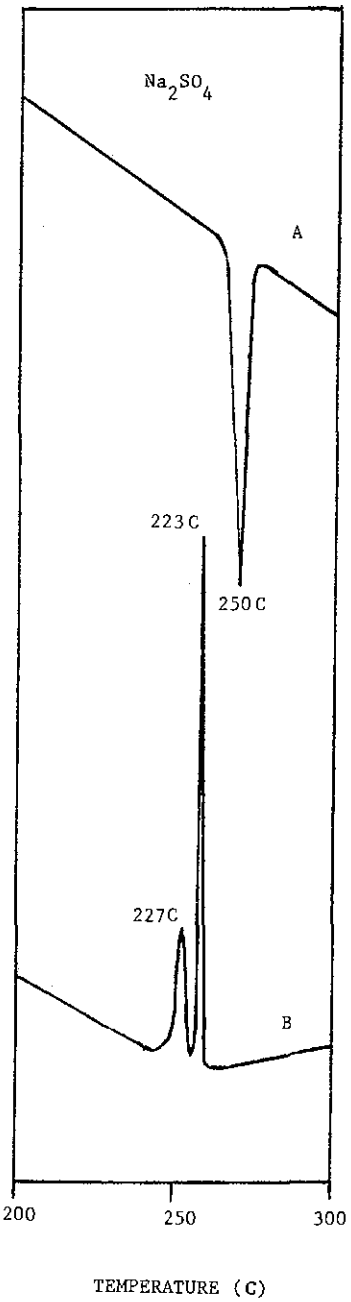

Figure 7 Differential scanning calorimetry curve for Na_2SO_4; A. heating; B. cooling (both A & B at 2C/min). Like TGA, DSC is an excellent method for quantitative examination while Raman spectroscopy provides a mechanistic explanation. Raman spectra recorded in conjunction with DSC are presented in Figure 8.

Solid state phase transitions

$Na_2SO_4 \cdot 10H_2O$ (Glauber salt) possesses properties of value to heat exchangers or solar heating units. Differential scanning calorimetry (DSC) indicated that $Na_2SO_4 \cdot 10H_2O$ dehydrates at 32C, goes through a phase change at 250C and melts at 888C. Thermogravimetric analysis confirmed the water weight loss and found no evidence for any oxidation or reduction reaction over the entire temperature range. Upon cooling, from 1000C to ambient, DSC detected phase transitions at 241C and 230C (Figure 7). Published references [25, 26] did not agree, however, on the number and temperature locations of phase transitions in Na_2SO_4 and $Na_2SO_4 \cdot 10H_2O$ [25, 26]. A most recent study [26] detected only one transition upon cooling. The temperature of the transition was not given.

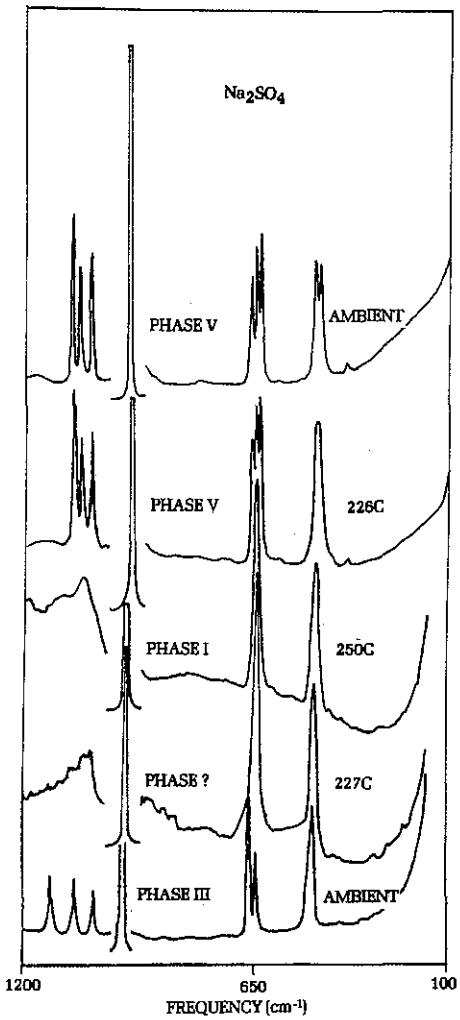

Figure 8 The Raman spectra of Na_2SO_4 as a function of tempereture provide a mechanistic understanding for the observed DSC phase transition behavior. See Table I for summary of DSC and Raman results.

TABLE I

The Phase Transition Behavior of $Na_2SO_4 \cdot 10\ H_2O$

[Ambient] —$Na_2SO_4 \cdot 10\ H_2O$→ [32C] —Na_2SO_4 (V), 10 C/min, See Note 1→ [250 C] —Na_2SO_4 (I)→ [884 C] melt

[Ambient] ←Na_2SO_4 (III), 5 C/min, See Note 2— [231 C] ←Phase?, See Note 3— [233C] ←Na_2SO_4 (I)

Na_2SO_4 (III) —2 C/min→ [246 C] —Na_2SO_4 (I)

[Ambient] ←Na_2SO_4 (III), 2 C/min— [227C] ←Phase ?, See Note 3— [232 C] ←Na_2SO_4 (I), 2 C/min

Note 1 - On first heating anhydrous Na_2SO_4 (V), a very small endotherm is observed at ~ 200°C, which does not reappear on cycling the sample. This endotherm is probably not due to a phase transition, but could be caused by the outgassing of H_2O or H_2SO_4.

Note 2 - The cooling rate is ~ 5 C/min.

Note 3 - Phase ? spectroscopically appears to contain frequencies from both phase I and phase III, with considerable disorder, phase ? was assigned as phase II by Kracek [25].

To confirm our DSC results, we recorded Raman spectra of Na_2SO_4 as a function of temperature (Figure 8). This was done in a simple but efficient manner by packing the powdered sample into a small, shallow cavity drilled into a soldering iron tip. The soldering iron was plugged into a Variac to control temperature and a thermocouple firmly secured to the copper tip to monitor temperature. The phase behavior of Na_2SO_4 obtained from Raman data (between 25C and 500C) was identical to that seen during our DSC study. A summary of the phase transitions observed is given in Table 1.

During the cooling cycle, a Na_2SO_4 phase was observed with Raman spectroscopy which was not reported by Davies and Sanford [26]. The spectral evidence for this conclusion was based upon the fact that the frequencies and band shapes of the symmetric and asymmetric stretches ($980cm^{-1}$ and $1120\text{-}1020cm^{-1}$ respectively), in the 241C to 230C temperature region, were different from those associated with known Na_2SO_4 crystal structures. The spectrum of this phase appears to be a combination of phase III and I with phase III being predominant (see Table 1 for phase designations). Considerable disorder is evident in the spectrum of this intermediate phase. Further Raman thermal studies will allow a better description to be presented, but our results clearly show that the intermediate phase is unique and that the spectrum is not caused by a temperature effect. Kracek [25] had previously suggested that a unique phase existed in this temperature range, based upon thermal evidence. Verification of the intermediate phase provides a mechanistic understanding of, and experimental evidence for, why phase III of Na_2SO_4 is found after heating $NaHSO_3$ instead of the expected phase V.

It should be noted that phase III is metastable at room temperature and will revert to phase V within a few months [26]. This process can be accelerated in the presence of moist air, or will take place spontaneously if Na_2SO_4 is converted to $Na_2SO_4 \cdot 10H_2O$. The production of anhydrous Na_2SO_4 (phase V) is then realized by dehydrating the $Na_2SO_4 \cdot 10H_2O$ at 32C.

Organic and organometallic phase transitions

Raman spectroscopy has proven beneficial in examining the solid-state phases of organics and organometallics. The rate of solubility, reaction rate, yield, beneficial industrial properties, etc of each chemical class can be markedly influenced by the crystal-phase properties. We have found, for instance, that syntheses of some organometallics are inhibited or accelerated depending upon the reactant's phase. Further, the phase of the organometallic compound produced is apt to change with only slight alterations in reaction temperatures, pressures, solvents, and the like.

NL Industries is presently relying on Raman spectroscopy as the principal method of analysis for organometallic antimony - ethylene glycol adducts and associated phases. The particular phase of commercial value will revert to an undesirable form rather easily, if production conditions are also not strictly adhered to. Because the spectra of the two forms are distinct, a Raman check of phase purity can be carried out in about twenty minutes. By contrast, infrared spectra of these two forms are rather similar, making it difficult to distinguish between them. The antimony oxygen bonds of the adduct are very weakly absorbing in the infrared, a further difficulty when trying to distinguish between adduct formation and unreacted mixtures. The infrared KBr pellet method is generally not suitable for infrared examination of organometallic samples since sample degradation is likely to occur.

Inorganic Analysis

In many cases Raman spectroscopy is analytically superior to the more common methods of inorganic compound analysis. Its advantages of speed, sensitivity, and accuracy can be readily applied to analyses of a wide variety of commercially important products. Two such applications are the analysis of $BaTiO_3$ and $TiCl_4$.

Raman spectroscopy was responsible for detecting a $CO\overline{\overline{3}}$ impurity, at ~1 weight %, in $BaTiO_3$ products. With Raman, and combined with other methods, we were able to prove that the presence of $CO\overline{\overline{3}}$ was caused by certain manufacturing conditions and that the $CO\overline{\overline{3}}$ was present as a coating on individual grains. The detection of this coating was especially significant because variations in dielectric properties and sintering characteristics of $BaTiO_3$ might be directly attributed to the number of particles coated and the thickness of the carbonate coating.

Titanium tetrachloride is a commercial intermediate in the manufacture of a number of chemical products. It is a very corrosive liquid which, unfortunately, liberates HCl on contact with moist air. Raman spectroscopy is especially valuable for analyzing such materials without exposure to air. This is accomplished by recording spectra throngh the side of the glass sample container. In this fashion we analyzed for CS_2, $TiOCl_2$ and $Ti(OH)_4$ in production batches of $TiCl_4$. The $TiCl_4$ spectrum consists of four sharp bands between $100\text{-}500cm^{-1}$ [27]. Here, impurity analysis at very low levels is simplified by the small number of bands and the absence of an interfering background throughout the spectral region of interest.

Raman spectroscopy can also record the vapor-phase spectrum above the $TiCl_4$ liquid, again in the same sealed container. The distribution coefficients between the vapor and liquid phase impurities can be determined without exposing the corrosive and reactive $TiCl_4$ to further contamination. The determination of distribution coefficients can lead to methods for impurity removal from this commercially important product.

Pilot plant trials

With speed, ease of sample preparation, and accuracy, Raman spectroscopy is ideal for monitoring pilot plant reactions. In numerous situations Raman spectroscopy will easily provide answers which, at best, would otherwise be difficult to acquire. As one such illustration, consider a reaction for producing metal bonded to sulfur type organometallics:

$$Z(R\text{-}S\text{-}H) + M^{Z+} \longrightarrow M(SR)_Z(\text{liquid}) + \text{side products}$$

Where: M = Metal cation
Z = 3 or 5
R = Organic reactant

The resulting M-S bonds produce strong stretching vibrations falling between 500 and $100cm^{-1}$ in the Raman spectrum. Based upon the number of spectral peaks, wavelengths and intensities, it is possible to distinguish between $M(SR)_3$ and $M(SR)_5$. For instance, pyramidal $M(SR)_3$ will produce two intense stretching bands, wheras $M(SR)_5$, the trigonal bipyramid, is expected to produce three intense stretching vibrations[28].

The major side product associated with these reactions is R – S – S – R, the mercaptide dimer. The – S – S – bond produces an intense S – S symmetric stretch falling at ~530-500cm^{-1}. The mercaptide, on the other hand, is characterized by a strong S – H stretch. By recording one Raman spectrum from 50 to $4000cm^{-1}$, the % S – H, the % S – S impurity, and % $M(SR)_Z$ data will all be available. The speed of this analysis allows results to be obtained every few minutes and pilot-plant conditions to be altered during a single run.

Quantitative data is obtained by adding ~ 5 weight % $CDCl_3$ to the reacting liquid, agitating for several minutes and then recording the spectrum of the sample in a 2mm diameter capillary. The height of the C – D stretch at ~2250cm^{-1} is

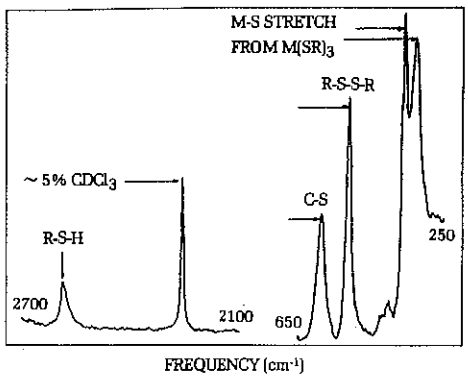

Figure 9 Raman spectra from pilot plant runs of an organometallic compound. The addition of 5% $CDCl_3$ served as an internal standard (the 250-650cm^{-1} region was recorded before addition of $CDCl_3$). Raman analysis proved to be extremely helpful during pilot plant scale-up studies.

compared to the S – H at ~2650cm^{-1}, the S – S at ~525cm^{-1}, and bands due to the M – S stretch from M(SR)3 and/or M(SR)5 (Figure 9).

A correction factor for dilution of one species by another can be included in the calibration curve. With Raman analysis, the S – H monomer, S – S dimer, $M(SR)_z$ and organometallics of unwanted oxidation states can be detected at 0.5 weight %. Because the method is so fast, we have been able to modify conditions during actual pilot trials to maximize yields. The influence of various catalysts has also been successfully studied in this manner.

Many industrial inorganic reactions are carried out in aqueous media, during which acetic acid is generated or consumed. Raman analysis can again be applied, with emphasis being placed on quantitative determination of acetic acid in water. To illustrate the technique, typical Raman curves of the C = O stretching and H_2O bending bands at 1720cm^{-1} and 1640cm^{-1}, respectively, are presented in Figure 10. The weak 1640cm^{-1} H_2O band is selected as an internal standard to normalize the C = O band of the acid, the 1640cm^{-1} band is then subtracted, the C = O band integrated and its area read off a SCAMP-generated calibration curve to yield % acetic acid. Acetic acid solntions as dilute as .1% can be determined by signal averaging, with errors of ± .01%. Figure 11 is a calibration curve. Total analysis time is ~ 10 minutes after calibration has been achieved. Thus, we were able to obtain results much faster than by classical wet methods.

Summary

The examples discussed above were selected to illustrate the speed, accuracy, ease of sample preparation, and sensitivity of Raman analysis for industrial analytical problems. One of the main advantages for an industrial analytical laboratory is the cost savings that can be realized. Obtaining the data in this article by techniques other than Raman spectroscopy would have significantly increased the cost of analysis.

Our illustrations of these advantages are by no means all inclusive; Raman analysis at NL Industries is also being applied to study the chemistry and phase stability of $BaTiO_3$ dielectrics, to distinguish between and quantitatively analyze mixtures of phosphorus/oxygen compounds, to examine aqueous solutions for organic and inorganic impurities, and to a number of other proprietary R&D projects.

And in addition to standard Raman spectroscopy, other inelastic light-scattering techniques, like resonance Raman, hyper-Raman, coherent anti-Stokes resonance Raman and Raman gain experiments may open up new vistas for chemical analysis. Their industrial applications are limited only by the availability of problems to solve and the imagination of the analyst to apply them.

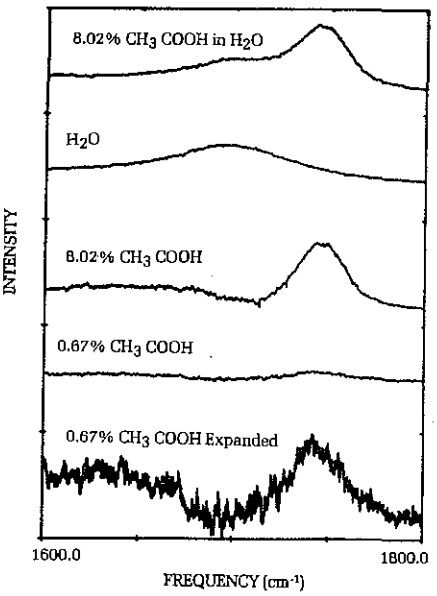

Figure 10 Raman date for acetic acid-water mixtures. The uppermost spectrum is of 8.02% acid in water. Below is the water background and next is the subtracted spectrum obtained by keystroke programming the SPEX SCAMP data system. The 0.67% acid spectrum, after subtraction, does not seem to show a band at ~1740cm^{-1}. However, when expanded vertically by the SCAMP, the band definitely appears above the background noise (lower most spectrum).

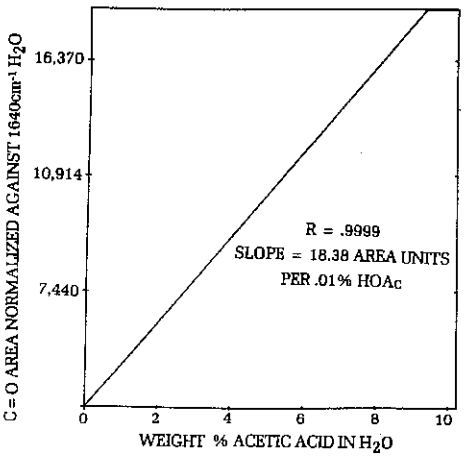

Figure 11 Corrected calibration curve for acetic acid in water obtained with Spex SCAMP and spectra in Figure 10. Experimental points lie under solid curve with a limit of detection well under 0.67% acetic acid.

REFERENCES

1. G. Herzberg, Infrared and Raman Spectra (Van Reinhold Co., New York, 1945)
2. S. Freeman Applications of Laser Raman Spectroscopy, (John Wiley and Sons, New York, 1974)
3. N. Colthrup, L. Daley and S. Wiberly, Introduction to Infrared and Raman Spectroscopy, (Academic Press, Inc., New York, 1975)
4. J.L. Koenig, Appl. Spectrosc. Rev. **4**, 233 (1971)
5. J.L. Koenig, Proc. Polym. Charact. Conf. 1974, **73-93**, Cleveland State University, Cleveland, Ohio
6. I.W. Sheperd, Adv. Infrered Raman Spec. **3**, 127 (1977)
7. J.F. Scott, The Spex Speaker, Vol. **XVII-2**, Spex Industries (1972)
8. C.A. Cody, R.C. Levitt, R.K. Khanma and P.J. Miller, J. Solid State Chem. **26**, 281 (1978) and **26**, 293 (1978)
9. P.S. Peercy and G.A. Samara, Phys. Rev. **B8 (5)**, 2033 (1973)
10. G.J. Thomas, The Spex Speaker, Vol. **XXI-4**, Spex Industries (1976)
11. T.G. Spiro, Vib. Spectra. Struct. **5**, 101 (1976)
12. C.H. Chow and G.J. Thomas, Biopolymers **16**, 765 (1977)
13. J. Loader, Basic Laser Raman Spectroscopy P. 45, (Heyden/Sadtler, 1970)
14. D. Thomas, Appl. Spectrosc. **31 (6)**, 515 (1977)
15. J. Nestor, J. Chem. Phys. **69**, 1778 (1978)
16. H. Remy, Treatise on Inorganic Chemistry, **Vol. II** Elsevier, New York, 1956, P. 665
17. K. Dihlstrom, Z. Anorg. Chem. **239**, 57 (1938)
18. E.J. Roberts and F. Fenwick, J. Am. Chem. Soc. **50**, 2125 (1928)
19. D.J. Stewart, O. Knop, C. Ayasse and F.W.D. Woodhams, Can. J. Chem. **50**, 690 (1972)
20. J.L. Waring, R.S. Roth, H.S. Parker and W.S. Brower, Mater. Res. Bull. **80A**, 761 (1976)
21. C.A. Cody, L. DiCarlo and R.K. Darlington, Inorg. Chem. **18 (6)**, 1572 (1979)
22. D. Rogers and A.C. Skapski, Proc. Chem. Soc. London, **400** (1964)
23. C.A. Cody, M.T. Hatcher, R.K. Darlington, 6th Annual FAACS Meeting, Philadelphia, Pa., September 16-21, 1979
24. R.J. Capwell, F. Spagnolo and M.A. DeSesa, Appl. Spectrosc. **26**, 537 (1972)
25. F.C. Kracek, J. Phys. Chem. **33**, 1281 (1929)
26. J.E.D. Davies and W.F. Sanford, J. Chem. Soc. Dalton Trans. 1912 (1975)
27. R.J.H. Clark, B.K. Hunter and D.M. Rippon, Inorg. Chem. **11**, 56 (1972)
28. K. Makamoto, Infrared and Raman Spectra of Inorganic and Coordination Compounds, (3rd Edition, John Wiley and Sons, New York, 1978) Chp. 2

The World Turns to SPEX for Spectrochemical Supplies

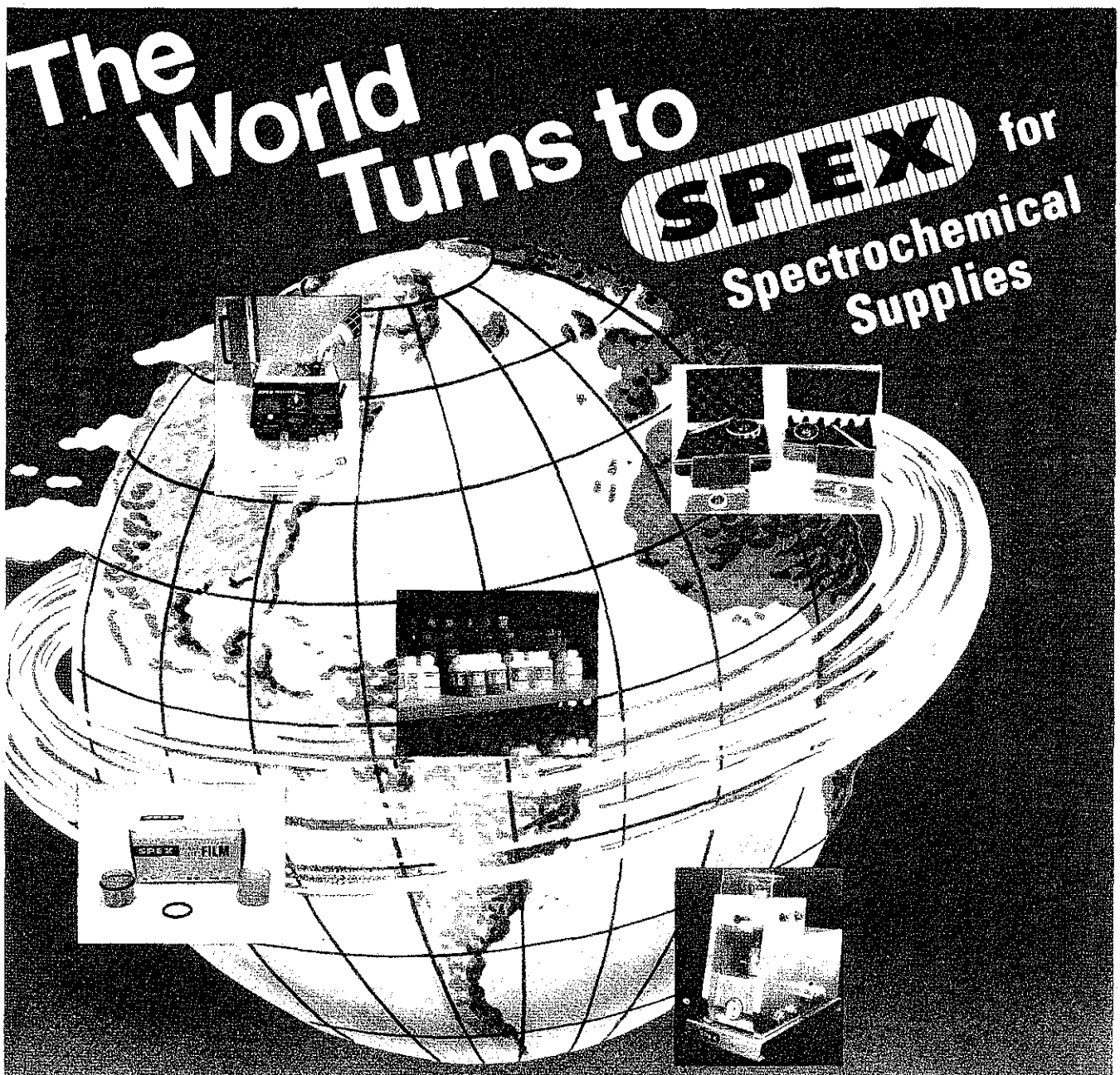

	AA	ICP/DCP	OES	IR	X-RAY	DTA/TGA
Aqueous and non-aqueous standards	x	x	x		x	
Powder standards			x		x	
PELLEMENT element standards					x	
X-PRESS hydraulic press				x	x	
SHATTERBOX, MIXER/MILL, FREEZER/MILL pulverizers			x	x	x	x
Mortar & pestles, boron carbide and silicon carbide			x	x	x	x
HiPure inorganics	x	x	x		x	
Expendable liquid cells					x	
Photographic plates			x			
Graphite electrodes			x			

and more; ASK FOR OUR CATALOG

We cross the 7 seas and 5 continents to destinations that circle the globe.

SPEX INDUSTRIES, INC.

P.O. Box 798
METUCHEN, NJ 08840
201-549-7144

WESTERN REGIONAL OFFICE
3246 McKINLEY DR.
SANTA CLARA, CA 95051
408-246-2333

SPEX INDUSTRIES, GmbH
IBLHERSTRASSE 53
D 8000 MUNCHEN 83
WEST GERMANY